

Gamma rays from Dark Matter Annihilation in Models of Radiative Neutrino Mass Generation

Talal Ahmed Chowdhury^{1,3} and Salah Nasri^{2,3}

¹Department of Physics, University of Dhaka, P.O. Box 1000, Dhaka, Bangladesh.

²Department of Physics, UAE University, P.O. Box 17551, Al-Ain, United Arab Emirates

³The Abdus Salam International Centre for Theoretical Physics, Strada Costiera 11, I-34014, Trieste, Italy.

Abstract

We present the Sommerfeld enhanced Dark Matter (DM) annihilation into gamma ray for a class of neutrino mass generation models with large electroweak multiplets where the neutrino mass is generated at one-loop and three-loop order. The DM candidates for one-loop and three-loop models are neutral scalar and fermion respectively and in both cases, the DM mass is in O(TeV) range. We show that in both models, the DM annihilation rate becomes more prominent for larger multiplets and it is already within the reach of currently operating Imaging Atmospheric Cherenkov telescopes (IACTs), High Energy Stereoscopic System (H.E.S.S.). Furthermore, Cherenkov Telescope Array (CTA), which will begin operating in 2030, will improve this sensitivity by a factor of $\mathcal{O}(10)$ and may exclude a large portion of parameter space of radiative neutrino mass models with scalar and fermionic DM of larger electroweak multiplet.

1. INTRODUCTION

In recent years, the gamma-ray observation by Cherenkov telescope has provided stringent and robust constraints for indirect detection and is also reaching the sensitivity level of DM annihilation cross sections to different Standard Model (SM) final states for the DM in $O(1 - 100)$ TeV mass range. Therefore, the latest result of H.E.S.S. (High Energy Stereoscopic System) for searching DM annihilation towards the inner galactic halo [1, 2] and the projected reach of CTA (Cherenkov Telescope Array) [3], can allow one to investigate the viability of a particular DM model with TeV mass.

Apart from the DM nature of the universe, the origin and smallness of the neutrino mass is yet to be concluded. A class of neutrino mass generation models ties these two issues together by radiatively generating neutrino mass¹ with DM particle running in the loop. Two prominent examples of this class of models are the Scotogenic model [4] where neutrino mass is generated at one-loop level and the Krauss-Nasri-Trodden (KNT) model [5] where the neutrino mass is generated at three-loop level. The DM candidate in the Scotogenic model can be either fermionic and/or scalar dark matter depending on region of parameter space. On the other hand, in the KNT model, the only option for DM candidate is neutral fermion as the possibility of scalar field being DM is excluded by the direct detection experiments. In our subsequent analysis, we have considered the scalar DM of the Scotogenic model and the fermionic DM of the KNT model.

As there is no symmetry reason to prevent extending the BSM field content of both scotogenic and KNT model with larger electroweak multiplets, we have used the gamma ray constraints coming from the DM annihilation rate which is greatly enhanced by the non-perturbative Sommerfeld enhancement induced by electroweak gauge bosons, which occurs for non-relativistic DM with mass $m_{DM} \gg m_W$, to determine the viability of models with larger multiplets.

2. THE MODEL

2.1. The Scotogenic Model

The scalar sector of the generalized scotogenic model has been presented in [7, 8]. The general Higgs-scalar potential that involves the $SU(2)_L$ scalar multiplet Δ with isospin, $J = n/2$ (n odd) and hyper-charge, $Y = 1/2$, symmetric under a Z_2 , is as follows,

$$V_0(H, \Delta) = -\mu^2 H^\dagger H + M_0^2 \Delta^\dagger \Delta + \lambda_1 (H^\dagger H)^2 + \lambda_2 (\Delta^\dagger \Delta)^2 + \lambda_3 |\Delta^\dagger T^a \Delta|^2 + \alpha H^\dagger H \Delta^\dagger \Delta + \beta H^\dagger \tau^a H \Delta^\dagger T^a \Delta + \gamma \left[(H^T \epsilon \tau^a H) (\Delta^T C T^a \Delta)^\dagger + h.c \right] \quad (1)$$

Here, τ^a and T^a are the $SU(2)$ generators in fundamental and Δ 's representation respectively. C is an antisymmetric matrix such that $CT^a C^{-1} = -T^{aT}$. Also H is the Higgs doublet and Δ is given as

$$\Delta_{\frac{n}{2}} = \left(\Delta_{\frac{n}{2}}^{(\frac{n+1}{2})}, \Delta_{\frac{n-2}{2}}^{(\frac{n-1}{2})}, \dots, \Delta_m^{(Q)}, \dots, \Delta_{-\frac{1}{2}}^{(0)} \right) \equiv \frac{1}{\sqrt{2}} (S + iA), \dots, \Delta_{-m-1}^{(-Q)}, \dots, \Delta_{-\frac{n}{2}}^{(-\frac{n-1}{2})} \Big)^T \quad (2)$$

¹For a review of radiative neutrino mass generation models, please see [6].

where the subscript is T_3 value and superscript is electric charge, $Q = T_3 + Y$.

The γ term in Eq. 1 is only allowed for representations with $(J, Y) = (\frac{n}{2}, \frac{1}{2})$ and splits the mass between scalar and pseudoscalar components of the neutral field at tree-level so that one can suppress the Z boson induced direct detection bound. Incidentally for complex odd dimensional $(J = n, Y \neq 0)$, $(n = 1, 2, \dots)$ scalar multiplets, γ term doesn't occur in the Z_2 symmetric scalar potential Eq. 1 and therefore, DM candidate is excluded by direct detection. Moreover, apart from the largest charged component ($T_3 = n/2$) of the multiplet, the γ term mixes the components with charge $|Q|$. Therefore, the corresponding mass eigenstates are $\{\Delta_m^{(Q)}, \Delta_{-m-1}^{(Q)}\} \rightarrow \{\tilde{\Delta}_1^{(Q)}, \tilde{\Delta}_2^{(Q)}\}$.

By setting S to be the DM candidate, one has the following mass hierarchy in the components,

$$m_S < m_{\tilde{\Delta}_1^+} < m_{\tilde{\Delta}_1^{++}} < \dots < m_{\tilde{\Delta}_1^{(Q)}} < \dots < m_{\tilde{\Delta}_2^{(Q)}} < m_{\tilde{\Delta}_2^+} < \dots < m_{\tilde{\Delta}_2^{(Q)}} < \dots < m_A \quad (3)$$

2.2. The KNT Model

The Beyond Standard Model (BSM) content of the model consists of two single charged singlet scalars, S_1^+, S_2^+ and three singlet RH neutrinos, N_{R_i} , $i = 1, 2, 3$ under SM gauge group with masses lie in the GeV-TeV range. Here, the lightest singlet RH neutrino N_{R_1} plays the role of DM. Subsequently, KNT model can be generalized [9] by replacing S_2^+ with Φ having integer isospin and hypercharge, $Y = 1$ and N_{R_i} with F_i that has integer isospin and $Y = 0$ under SM gauge group. In the generalized KNT model, the lightest neutral fermion component, F_1^0 is the viable DM candidate. Such replacement in KNT model with large electroweak multiplets have been studied for triplet [10], 5-plet [11] and 7-plet [12] cases. In [13], we have investigated the charged lepton flavor violating processes in the generalized KNT model. In this work we focus on 5-plet and 7-plet cases because the Z_2 symmetry, $\{S_2^+, N_{R_i}\} \rightarrow \{-S_2^+, -N_{R_i}\}$ needed to prevent the Dirac neutrino mass term in the Lagrangian, is not required anymore for larger multiplets like in 5-plet and 7-plet cases.

Apart from the SM field content, we add the following BSM fields in the generalized KNT model which are charged under SM gauge group, $SU(3)_c \times SU(2)_L \times U(1)_Y$ as

$$\text{Complex scalars : } S_1^+ \sim (0, 0, 1), \quad \Phi \sim (0, j_\phi, 1), \quad \text{and Real fermions : } F_{1,2,3} \sim (0, j_F, 0) \quad (4)$$

where j_ϕ and j_F are integer isospin of $SU(2)_L$.

In this comparative study, we focus on two set of models in this class; 5-plet model: $\Phi \sim (0, 2, 1)$ & $F_{1,2,3} \sim (0, 2, 0)$ and 7-plet model: $\Phi \sim (0, 3, 1)$ & $F_{1,2,3} \sim (0, 3, 0)$.

The SM Lagrangian is augmented in the following way,

$$\mathcal{L} \supset \mathcal{L}_{SM} + \{f_{\alpha\beta} \bar{L}_\alpha^c \cdot L_\beta S_1^+ + g_{i\alpha} \bar{F}_i \cdot \Phi \cdot e_{\alpha R} + h.c\} - \frac{1}{2} \bar{F}_i^c M_{F_{ij}} F_j - V(H, \Phi, S_1) + h.c \quad (5)$$

where, c denotes the charge conjugation and dot sign, in shorthand, refers to appropriate $SU(2)$ contractions. Also L_α and e_{R_α} are the LH lepton doublet and RH charged leptons respectively and Greek alphabet α stands for generation index. Moreover, $[F]_{\alpha\beta} = f_{\alpha\beta}$ and $[G]_{i\alpha} = g_{i\alpha}$ are 3×3 complex antisymmetric and general complex matrices respectively. Finally, H denotes the SM Higgs doublet.

The scalar potential is given by,

$$V(H, \Phi, S_1) = V(H) + V(\Phi) + V(S_1) + V_1(H, \Phi) + V_2(H, S_1) + V_3(\Phi, S_1) \quad (6)$$

The three-loop neutrino mass generation and the DM stability depend on the V_3 term of Eq.(6). Explicitly the relevant terms of V_3 for 5-plet and 7-plet models are,

$$V_3^{(5)} \supset \frac{\lambda_S}{4} (S_1^-)^2 \Phi_{abcd} \Phi_{efgh} \epsilon^{ae} \epsilon^{bf} \epsilon^{cg} \epsilon^{dh} + \lambda_{S_1^-} \Phi^{*abcd} \Phi_{abef} \Phi_{cdjl} \epsilon^{ej} \epsilon^{fl} + h.c \quad (7)$$

$$V_3^{(7)} \supset \frac{\lambda_S}{4} (S_1^-)^2 \Phi_{abcdef} \Phi_{ghijkl} \epsilon^{ag} \epsilon^{bh} \epsilon^{ci} \epsilon^{dj} \epsilon^{ek} \epsilon^{fl} + h.c \quad (8)$$

Here the λ term in Eq.(7) is not invariant under Z_2 and eventually induce the decay of F_1^0 where the width is $\Gamma_{DM} \sim \lambda^2$. But, as pointed out in [11], the bound on DM mean life-time sets λ to be very small, and in the limit when $\lambda \rightarrow 0$, the Z_2 symmetry emerges. On the other hand, the λ term is absent in Eq.(8) because $j_\phi \otimes j_\phi$ contains symmetric (antisymmetric) irreducible representation with same isospin T_ϕ for even (odd) integer isospin which is further contracted with Φ^\dagger to obtain a singlet. So, for two identical scalar multiplets, the antisymmetric combination is zero and hence no λ term for $j_\phi = 3$.

As pointed out in [13], the mass splittings among component fields of the scalar multiplet is controlled by $\lambda_{H\phi 2} (\Phi^\dagger \cdot H) \cdot (H^\dagger \cdot \Phi) \subset V_2$ term after electroweak symmetry breaking and allowed splittings only lead to $\Delta m_{ij}^2 / M_0^2 \sim 10^{-3}$ for invariant mass of the scalar multiplet, $M_0 = 10$ TeV and the ratio becomes smaller for $M_0 > 10$ TeV. On the other hand, the mass splittings in fermionic component fields are zero at tree-level and only receive $O(100)$ MeV splittings due to radiative correction after electroweak symmetry breaking [14]. Therefore such scenario can be considered as the near-degenerate case.

In the generalized KNT model, the lightest neutral component of the fermion multiplet, F_1^0 is the viable DM candidate. In comparison, the neutral component of the scalar multiplet, $\phi^0 = \frac{1}{\sqrt{2}}(S + iA)$ could have provided S to be DM but it is ruled out as

it induces Z-mediated dark matter nucleon scattering of the order 10^{-39} cm^2 which is much larger than the exclusion limit set by the direct detection experiments [24]. One can avoid this DM-nucleon scattering channel if the splitting between S and A is large enough to make this scattering kinematically forbidden but there is no renormalizable term in the Lagrangian which can induce such splitting in a generic way. Still, higher dimensional operator can split the S and A component [17] but then it is needed to address the UV completion of the model. Therefore, we restrict ourselves only to the renormalizable Lagrangian, and therefore the DM candidate is set to F_1^0 .

3. SOMMERFELD ENHANCED DM ANNIHILATION RATE

When the DM is non-relativistic, $v_{DM} \ll c$ and $m_{W,Z} \ll m_{DM}$, the exchange of massive W and Z gauge bosons between DM components will induce Yukawa potential and γ exchange will induce Coulomb potential which in turn significantly modifies the wavefunction of the incoming DM states and enhances the annihilation cross-sections. This phenomenon is known as Sommerfeld Enhancement (SE). The calculation of Sommerfeld enhanced DM annihilation cross section is well studied subject so here we follow the prescriptions given in [16, 17]. In the following we briefly review them to set up our notation for both the scotogenic and KNT models.

The Sommerfeld enhancement takes place in DM (co)annihilation processes with final states W^\pm , Z and γ bosons so we only consider the 2-particle states which are CP-even and have total charges $Q = 0, \pm 1, \pm 2$. These 2-particle states consist of component fields of the electroweak multiplet that contains the DM candidate. In the case of DM annihilation in the galaxy halo at present times, only 2-particle states with $Q = 0$ are relevant.

The modification of the wavefunction is determined by solving the radial Schrodinger equation with effective potential,

$$\frac{d^2 \Psi_{jj',ii'}}{dr^2} + \left[\left((m_{DM}v)^2 - \frac{l(l+1)}{r^2} \right) \delta_{jj',kk'} - m_{DM} V_{jj',kk'} \right] \Psi_{kk',ii'} = 0 \quad (1)$$

where r is the magnitude of the relative distance between two component fields in their center-of-mass frame, the kinetic energy of the incoming DM states, i.e. $|ii' = DMDM\rangle$ is $E = m_{DM}v^2$, The wavefunction $\Psi_{jj',ii'}$ gives the transition amplitude from $|ii'\rangle$ states to $|jj'\rangle$ states in the presence of effective potential, V .

We primarily focus on the S-wave annihilation so we set $l = 0$ and have

$$\frac{d^2 \Psi_{jj',ii'}}{dr^2} + \left[k_{jj'}^2 \delta_{jj',kk'} + m_{F_1} \left(\frac{f_{jj',kk'} \alpha_a e^{-n_a m_W r}}{r} + \frac{Q_{kk'}^2 \alpha_{em}}{r} \delta_{jj',kk'} \right) \right] \Psi_{kk',ii'} = 0 \quad (2)$$

Here, $k_{jj'}^2 = m_{DM}(m_{DM}v^2 - d_{jj'})$ is the momentum associated with the 2-particle state, $|jj'\rangle$ and $d_{jj'} = m_j + m_{j'} - 2m_{DM}$ denotes the mass differences between DM and other states of the multiplet. $Q_{kk'}$ is the electric charge associated with state $|kk'\rangle$. Also, $\alpha_W = \alpha$ and $n_W = 1$ for W boson exchange and $\alpha_Z = \alpha / \cos^2 \theta_W$ and $n_Z = 1 / \cos \theta_W$ for Z boson exchange. Finally, $f_{jj',kk'}$ is the group theoretical factor associated with $SU(2)$.

Now by using dimensionless variables defined as $x = \alpha m_{DM} r$, $\epsilon_\phi = (m_W / m_{DM}) / \alpha$, $\epsilon_v = (v/c) / \alpha$ and $\epsilon_{d_{ii'}} = \sqrt{d_{ii'} / m_{DM}} / \alpha$, we re-write the coupled radial Schrodinger equations as

$$\frac{d^2 \Psi_{jj',ii'}}{dx^2} + \left[\hat{k}_{jj'}^2 \delta_{jj',kk'} + \frac{f_{jj',kk'} n_a^2 e^{-n_a \epsilon_\phi x}}{x} + \frac{Q_{kk'}^2 \sin^2 \theta_W}{x} \delta_{jj',kk'} \right] \Psi_{kk',ii'} = 0 \quad (3)$$

where the dimensionless momentum, $\hat{k}_{jj'}^2 = \epsilon_v^2 - \epsilon_{d_{ii'}}^2$.

At large x , $\Psi_{jj',ii'}$ behaves as $\Psi_{jj',ii'} \sim T_{jj',ii'} e^{i\hat{k}_{jj'} x}$ where $T_{jj',ii'}$ is the transition amplitude provided the effective potential is dominated by Yukawa potential. Now if the annihilation matrix for final state f is given by $\Gamma_{jj',ii'}^{(f)}$, the annihilation cross section is,

$$\sigma_{DMDM \rightarrow f} = c(T^\dagger \cdot \Gamma^{(f)} \cdot T)_{DMDM, DMDM} \quad (4)$$

where $c = 2$ for $|DMDM\rangle$ state as it consists of identical fields.

The Scotogenic Model 2-states

In the scotogenic model, the DM-DM 2-particle state, $|SS\rangle$, is charge neutral and CP-even state hence it only mixes with other $Q = 0$ CP-even 2-particle states. Therefore, the 2-particle state vector with only charge neutral and CP even component, is given by

$$|\Phi_{\Delta_{\frac{3}{2}}}\rangle = \left(SS, AA, \Delta^{(\frac{n+1}{2})} \Delta^{(-\frac{n+1}{2})}, \dots, \tilde{\Delta}_1^{(Q)} \tilde{\Delta}_1^{(-Q)}, \tilde{\Delta}_2^{(Q)} \tilde{\Delta}_2^{(-Q)}, \dots, \tilde{\Delta}_1^{(Q)} \tilde{\Delta}_2^{(-Q)}, \tilde{\Delta}_2^{(Q)} \tilde{\Delta}_1^{(-Q)}, \dots, \tilde{\Delta}_2^{(\frac{n-1}{2})} \tilde{\Delta}_1^{(-\frac{n-1}{2})} \right)^T \quad (5)$$

Here, the ordering of the components in the vector is arbitrary. One can adopt different ordering for convenience.

The KNT model 2-particle states

In the case of the KNT model, we have considered $M_{F_1} < M_{F_{2,3}}$, therefore only component fields of F_1 multiplet enter into 2-particle states as the fields of $F_{2,3}$ will be too heavy to couple with 2-particle states consist of F_1 's field components. We define 2-particle state vector corresponding to F_1 as

$$Q = 0: \quad |\Psi\rangle = (F_1^0 F_1^0, F_1^\pm F_1^\mp, F_1^{\pm\pm} F_1^{\mp\mp}, F_1^{\pm\pm\pm} F_1^{\mp\mp\mp} \dots)^T \quad (6)$$

$$Q = \pm 1: \quad |\Psi\rangle = (F_1^0 F_1^\pm, F_1^{\pm\pm} F_1^\mp, F_1^{\pm\pm\pm} F_1^{\mp\mp} \dots)^T \quad (7)$$

$$Q = \pm 2: \quad |\Psi\rangle = (F_1^0 F_1^{\pm\pm}, F_1^\pm F_1^\pm, F_1^{\pm\pm\pm} F_1^\mp \dots)^T \quad (8)$$

Again the ordering of the component 2-particle states, as above, is arbitrary.

Now we can solve the radial schrodinger equation in the presence of the matrix potential induced by the exchange of W , Z and γ to calculate the transition amplitude $T_{ii',jj'}$ and eventually the Sommerfeld enhanced cross-section for DM annihilation to final states, $f = WW, ZZ, \gamma\gamma, \gamma Z$ using Eq.(4).

4. DARK MATTER CONSTRAINTS

We have used the DM relic density and the direct detection bound to identify the viable parameter space of the DM candidate in the scotogenic and the KNT model. They are discussed at length in the following sections.

4.1. The Scotogenic Model with Large Electroweak Multiplet

4.1.1. DM relic density in the Scotogenic model

The relic density of the dark matter in the universe is measured by Planck collaboration as $\Omega_{DM} h^2 = 0.1197 \pm 0.0022$ (68% C.L.) [18]. If scalar DM of the scotogenic model is the dominant component of the DM, this relic density can be achieved either by thermal freeze-out or non-thermal process. For scalar DM, the thermal freeze-out processes are controlled by gauge and scalar interactions and proceed via the DM (co)annihilation into SM particles (for TeV scale DM, mostly into WW and ZZ). It was shown in [19] for doublet and [7] for quartet that, certain bounds on mass splittings between the DM and other components of the scalar multiplet are to be satisfied so that scalar DM can have the correct relic density. One can also expect Sommerfeld enhancement of the (co)annihilation processes involved in thermal freeze-out. But as shown in [20], for the freeze-out temperature, T_F , such that $m_S/T_F \sim 20$ (the typical freeze-out condition), the SE correction is not numerically significant and it only becomes important when $m_S/T_F \gtrsim 100$. Moreover it has been argued in [21, 22] that the exclusion of SE in the thermal freeze out will modify the relic density at most by 30%.

4.1.2. DM Direct Detection in Scotogenic Model

In the scotogenic model, the elastic scattering of DM with nucleus is induced by the higgs exchange and thus controlled by the coupling λ_S given in Eq.(??). The spin independent cross section is given by,

$$\sigma_{SI} = \frac{\lambda_S^2 f^2}{4\pi} \frac{\mu^2 m_n^2}{m_h^4 m_S^2} \quad (1)$$

Here, $\mu = m_n m_S / (m_n + m_S)$ is the DM-nucleon reduced mass. f parameterizes the nuclear matrix element, $\sum_{u,d,s,c,b,t} \langle n | m_q \bar{q} q | n \rangle \equiv f m_n \bar{n} n$ and from recent lattice results [23] $f = 0.347131$.

The LUX 2016 [25] result has put limit on the $m_S - \lambda_S$ plane as shown in Fig. 1 (left) and it can be seen that the direct detection experiments are reaching the sensitivity to probe dark matter in the high mass regime. Moreover the projected XENON 1T [26] can put stringent limit, if DM is not observed, on the $m_S - \lambda_S$ plane and will reach the one loop corrected cross section of the order $O(10^{-48} - 10^{-47} \text{ cm}^2)$ by W and Z bosons (as shown for the doublet in [27]) even if λ_S is tuned to be very small.

These direct detection limits also have important implications on the thermal freeze-out process in the scotogenic model. As we can see from Fig. 1 (right) that LUX 2016 has already probed 1 – 5 TeV and 1 – 7.5 TeV region for doublet and quartet respectively. Here we have taken into account the $O(30\%)$ modification in the relic density for not considering SE correction in freeze-out. Finally, the entire thermal freeze-out region for both doublet and quartet is enclosed by the XENON1T sensitivity limit.

4.2. The Generalized KNT Model

4.2.1. DM Relic Density in the KNT Model

The fermionic DM in the generalized KNT model can achieve the relic density either by the thermal freeze-out process or non-thermal process as we will describe below.

Thermal Freeze-out of DM. The thermal freeze-out of fermionic DM of the 5-plet and 7-plet, both proceed mainly through

- gauge interactions in dominant S -wave and sub-dominant P wave channels as the DM is non-relativistic and they are controlled by gauge coupling g and receive non-negligible Sommerfeld enhancement in mainly S -wave annihilation cross-sections.

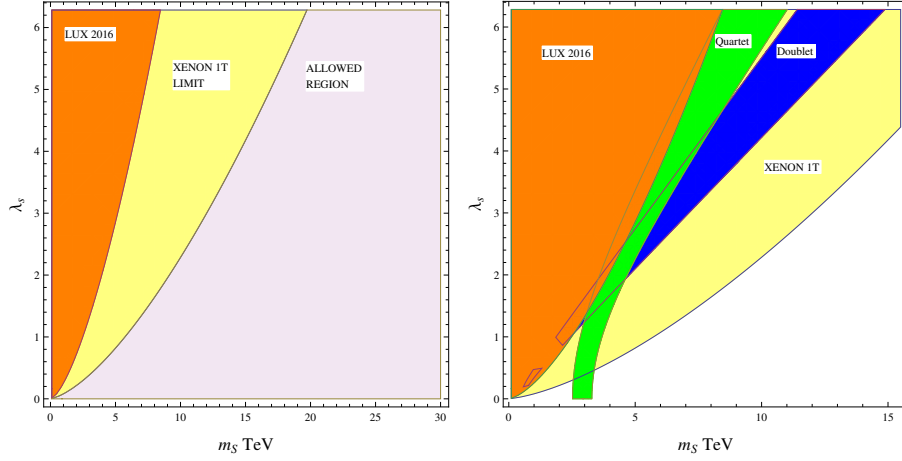


FIGURE 1: (Left) LUX(2016) exclusion limits and XENON 1T projected limits on $m_S - \lambda_S$ plane. (Right) Allowed region on $m_S - \lambda_S$ plane set by DM relic density for doublet (blue region) and quartet (green region). We can see that XENON 1T is already sensitive to both regions allowed by the DM relic density

- yukawa interactions in sub-dominant P -wave channels which are controlled by $g_{i\alpha}$ couplings and are less significant because of large gauge annihilation as pointed out in subsequent discussion.

The set of parameters of KNT model which enters into DM relic density calculation via thermal freeze-out, is $\{M_{F_1}, M_\phi, g_{1\alpha}\}$. On the other hand, the generalized KNT model describes the generation of the neutrino mass so, as described in [13], we scan over $M_{F_1} \in (1, 50)$ TeV, $M_{F_{2,3}} \in M_{F_1} + (1, 10)$ TeV, $M_\phi \in (10, 100)$ TeV, $m_S \in (500 \text{ GeV}, 50 \text{ TeV})$ and $\lambda_S \in (0.001, 0.1)$, with the numerical values of the yukawa couplings, $f_{\alpha\beta}$ and $g_{i\alpha}$, chosen to satisfy the low energy neutrino constraints [15]. For this reason, although the parameters, $M_{F_2}, M_{F_3}, g_{2\alpha}, g_{3\alpha}, f_{\alpha\beta}, m_S, \lambda_S$ do not enter into the DM analysis, they fix the parameter values $M_{F_1}, M_\phi, g_{1\alpha}$ so that the neutrino constraints are also satisfied at each point of the relevant parameter space of the KNT model.

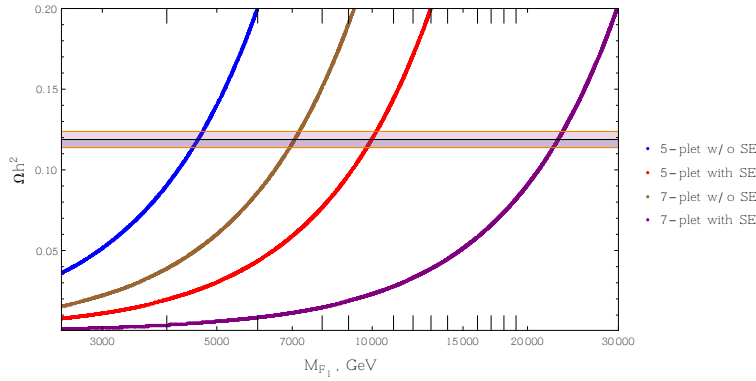


FIGURE 2: The DM relic densities, Ωh^2 of 5-plet w/o SE (blue), 5-plet with SE (red), 7-plet w/o SE (brown) and 7-plet with SE (purple) respectively. The horizontal band represents 5σ band with central value $\Omega h^2 = 0.1186 \pm 0.001$ measured by Planck.

Non-thermal Production of the DM. Apart from thermal freeze-out of DM which is mainly controlled by the gauge interactions, it is possible to set the DM relic density non-thermally by the out-of-equilibrium decay of ϕ scalar via $\phi^+ \rightarrow F_1^0 e_R^+$ in generalized KNT model. But as both Φ and F_1 are charged under the gauge group, the processes $\phi_i \phi_j \leftrightarrow VV$ and $F_i F_j \leftrightarrow VV$ will keep them in the thermal equilibrium. Therefore, one important condition is that the temperature where the decay takes place must be smaller than the temperatures where the gauge reactions of Φ and F_1 decouple.

From Fig. 3, we can see that the gauge reaction densities of Φ component fields, γ_ϕ , decouple when temperature becomes small. On the other hand, the decoupling of the inverse decay process $F_1^0 e_R^+ \rightarrow \phi^+$ which would deplete the amount of F_1^0 , is necessary. This condition sets the corresponding decay width, Γ_ϕ to be very small, at the order of $\sim 10^{-18}$ GeV so that the inverse process remains decoupled throughout the whole thermal history of the universe as shown in the Fig. 4 (left).

Besides, Fig. 4 (right) represents the $\delta - |g_{1\alpha}|$ plane bounded by the constraint $\Gamma_\phi \lesssim 10^{-18}$ GeV so that the inverse decay process remains out of equilibrium during the thermal evolution of the universe. We can see that, such small decay width of ϕ^+ implies that the mass difference between ϕ^+ and F_1^0 needs to be of the order $\mathcal{O}(1 - 10)$ MeV and $|g_{1\alpha}| \sim 10^{-4}$ for $M_\phi \sim 10$ TeV. Therefore from this estimates, we can infer that the out-of-equilibrium decay of ϕ^+ to generate DM content of the universe only holds for

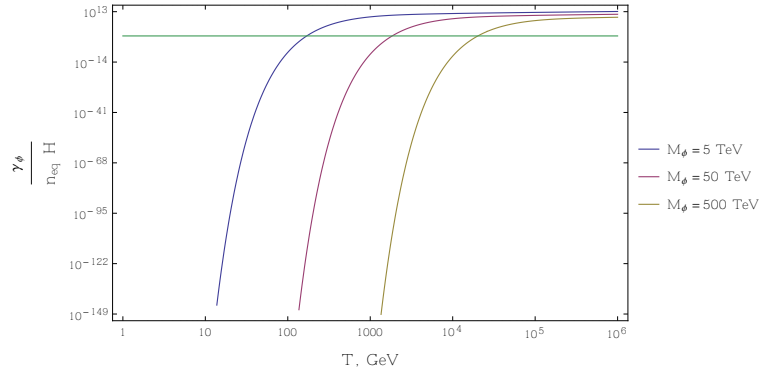


FIGURE 3: Decoupling of the gauge reaction densities, γ_ϕ of Φ with temperature. Here the green horizontal line represents, $\frac{\gamma_\phi}{n_{\text{eq}} H} = 1$ where the processes $\phi_i \phi_j \leftrightarrow VV$ due to gauge interaction are decoupled.

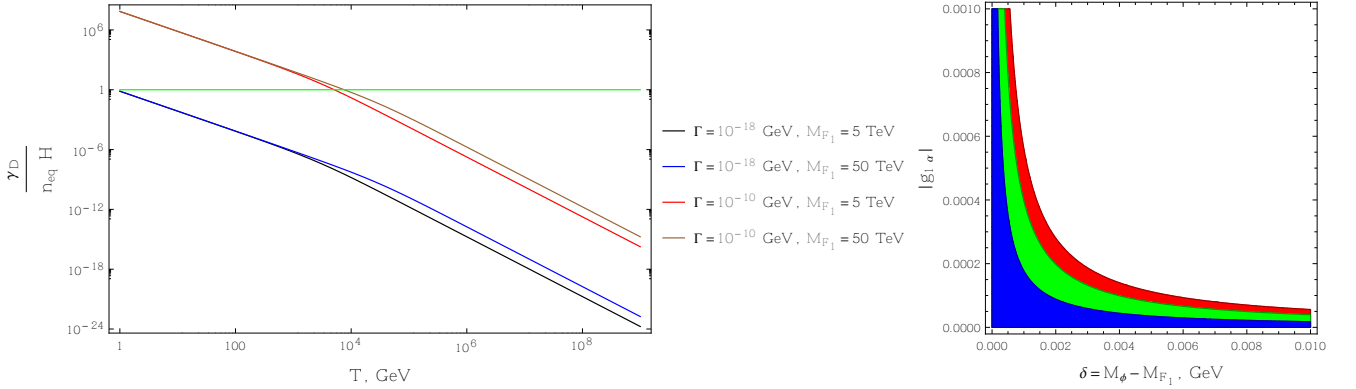


FIGURE 4: (left) Decoupling of inverse decay process with temperature and (right) Allowed region in $\delta = M_\phi - M_{F_1}$ vs $|g_{1\alpha}|$ plane due to $\Gamma_\phi \leq 10^{-18}$ GeV for $M_\phi = 10$ TeV (blue), $M_\phi = 50$ TeV (green), $M_\phi = 100$ TeV (red) respectively.

a fine-tuned parameters of the model. Nevertheless, one can extend the generalized KNT model with another sector which can non-thermally produce the DM without any fine-tuning.

4.2.2. DM Direct Detection in The KNT Model

The DM candidate F_1^0 does not couple to quarks at tree-level because of its vanishing hypercharge. However at one loop level, due to exchange of W boson, it has effective coupling with the quarks which leads to both spin-dependent and spin-independent contribution in DM-nucleon scattering. The spin-dependent cross-section is suppressed by the mass of the DM which is at $O(\text{TeV})$. On the other hand, the spin-independent cross-section for fermionic multiplet with integer isospin j , which doesn't depend on the DM mass, is given by [14],

$$\sigma_{SI} = j^2(j+1)^2 \frac{\pi \alpha^2 M_{\text{Nucl}}^4 f^2}{4m_W^2} \left(\frac{1}{m_W^2} + \frac{1}{m_h^2} \right) \quad (2)$$

where, M_{Nucl} is the mass of the target nucleus, f parametrizes nucleon matrix element as $\langle n | \sum_q m_q \bar{q}q | n \rangle = f m_n \bar{n}n$ and from lattice result, $f = 0.347131$ [23].

5. RESULT AND DISCUSSION

5.1. The Scotogenic Model

In the case of scalar DM of the scotogenic model, the mass splitting between the DM and the charged state of the multiplet can be sizable and eventually suppress the Sommerfeld enhancement.

We have determined the cross sections for two cases. The first case is the (almost) degenerate limit, where the mass splittings among the components of the scalar multiplet, are set to their minimum values and the second case is the maximal mass splitting limit where the mass splittings are set at their maximum values where both values are allowed by the constraints on Electroweak Precision Observables, DM relic density and DM direct detection. In addition, the LUX direct detection limit [25] and XENON1T sensitivity limit [26] fix two maximal mass splitting sets for the doublet, referred as LUX2016 and XENON1T respectively in the Fig. 6. The detailed description of the relevant constraints, viable parameter space and the results can be found in the paper [17].

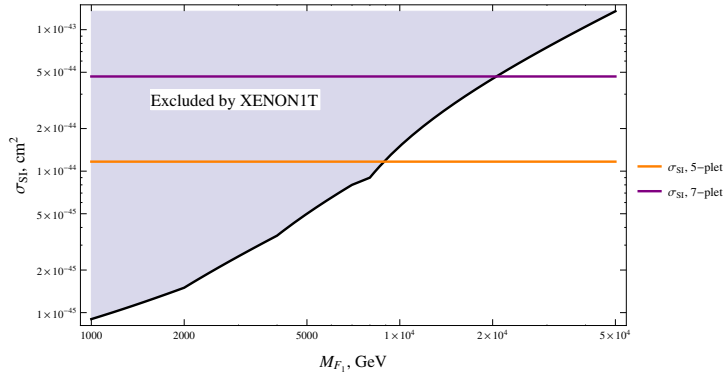


FIGURE 5: Spin-independent cross section of DM-nucleon interaction. The shaded region is excluded by XENON1T (2017) data [24]. The exclusion limit on DM mass in [24] is given up to 10 TeV. Here we have extrapolated this exclusion limit up to 50 TeV. As we can see, the thermal DM scenario with $M_{F_1} = 9.9$ TeV for 5-plet and $M_{F_1} = 22.85$ TeV for 7-plet, are almost at the verge of exclusion by the XENON1T (2017).

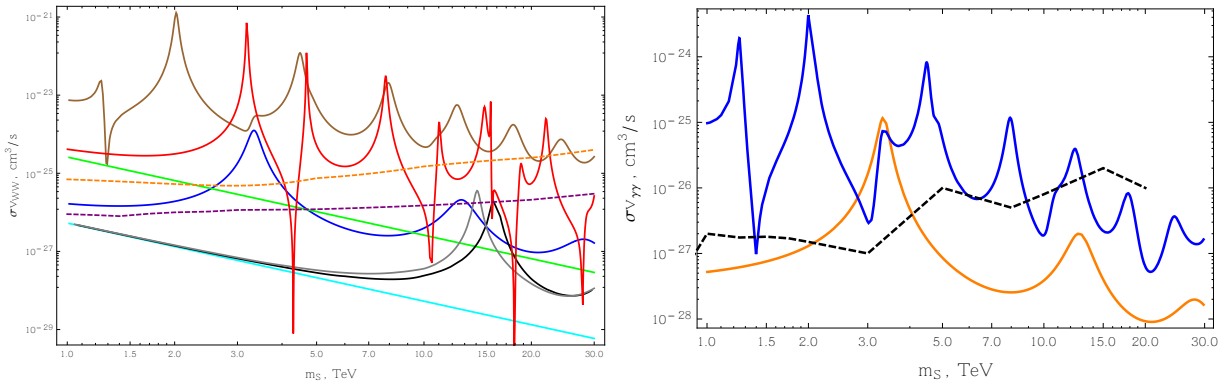


FIGURE 6: In the left fig. correlation between σv_{WW} and m_S . The blue (doublet) and brown (quartet) lines represent the annihilation cross section to WW in the (almost) degenerate limit. The black (doublet, LUX2016), grey (doublet, XENON1T) and red (quartet) lines represent the cross section when mass splittings are taken as the maximum of allowed limit. The light blue (doublet) and green (quartet) lines are the tree-level annihilation cross sections. Moreover, the orange and purple dashed lines are H.E.S.S. and future CTA limits respectively on WW annihilation. In the right fig. correlation of $\sigma v_{\gamma\gamma}$ with m_S for the doublet (orange line) and quartet (blue line) cases at the almost degenerate limits. Also the black dashed line in left fig is the H.E.S.S. limits on $\gamma\gamma$ annihilation.

In this study we have demonstrated that the Sommerfeld enhancement of the DM annihilation cross section increases with the size of the scalar multiplet but in the case of larger multiplet resonance dips or suppression for certain values of the DM mass appear along with resonances.

Consequently large Sommerfeld enhanced DM annihilation cross section have important implications on the indirect detection. We can see from Fig. 6 (left) that H.E.S.S. has already achieved the sensitivity to probe the entire 1 – 30 TeV mass range for the quartet except $m_S \sim 27$ TeV for the (almost) degenerate limit and dips at certain mass values for the allowed maximum mass splitting. On the other hand, for the doublet, except for 2.5 – 4 TeV for (almost) degenerate limit and almost all of 1 – 30 TeV for allowed maximum limit, are below the H.E.S.S. limit. Future CTA sensitivity limit is improved by $O(10)$ compared to H.E.S.S. limits.

For $SS \rightarrow \gamma\gamma$ case, the Sommerfeld enhanced cross section is obtained only for (almost) degenerate limit because maximum allowed mass splitting suppress the $T_{SS,jj}$, $jj = \tilde{\Delta}_j^{(Q)} \tilde{\Delta}_j^{(-Q)}$ factors and thus annihilation becomes negligible. For such case, the $\gamma\gamma$ and γZ annihilation proceed through one loop process via charged scalars exchange and has $10^{-32} - 10^{-27} \text{ cm}^2 \text{ s}^{-1}$ for doublet and quartet. From Fig. 6 (right), we can see that H.E.S.S. limit can already probe 1 – 9 (except for dip at 1.4 TeV) and 11.5 – 14 TeV of their considered 1 – 20 TeV mass range for the quartet whereas for the doublet only 2.1 – 4.1 TeV out of 1 – 20 TeV is within the reach of H.E.S.S.

5.2. The Generalized KNT Model

In this section we present the Sommerfeld enhanced DM annihilation cross-sections in the generalized KNT model; $F_1^0 F_1^0 \rightarrow W^+ W^-$ and $F_1^0 F_1^0 \rightarrow \gamma\gamma$ which are sensitive to IACTs. Once more, in the analysis we set, $v_{DM} = 10^{-3}$ which is the scale of DM average velocity in the galactic halo.

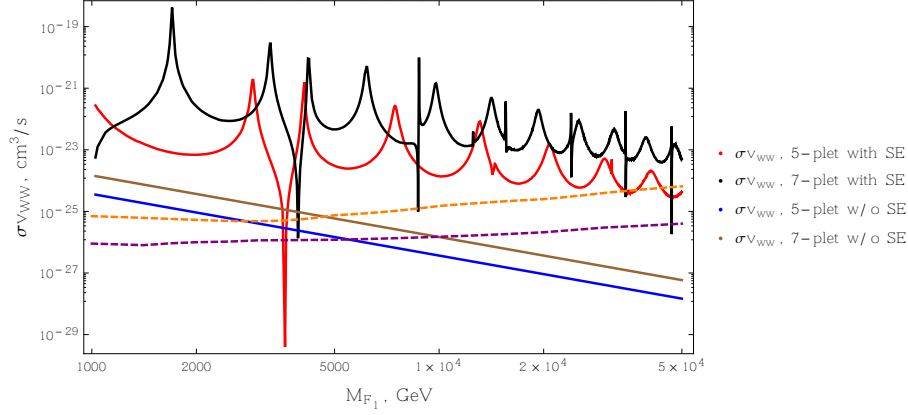


FIGURE 7: Sommerfeld enhanced cross-section σv_{ww} at the galactic halo of the Milky Way for 5-plet (red) and 7-plet (black). Moreover, σv_{ww} without SE is given for 5-plet (blue) and 7-plet (brown). Here orange and purple dashed lines are H.E.S.S observed limit and CTA sensitivity limit on σv_{ww} respectively

In Fig. 7, we can see the resonance and dips occurring for both 5-plet (red) and 7-plet (black) at particular mass values of DM due to SE in the presence of Yukawa potential induced by the exchange of massive W and Z bosons in the limit of non-relativistic velocity. Apart from the dips at 3.8 TeV (5-plet) and 4 TeV (7-plet), σv_{ww} is larger than its tree-level value (blue and brown lines for 5-plet and 7-plet respectively) for almost all of the DM mass range, 1-50 TeV. In fact for this mass range, it is large enough to be almost excluded by the H.E.S.S. limit (orange dashed line) provided that the F_1^0 is the dominant DM of the universe and follows the Einasto density profile [1]. In addition we can see from Fig. 7 that the future CTA will improve the exclusion limit by a factor of $\mathcal{O}(10)$ (purple dashed line) [3].

In addition, Fig. 8 represents the Sommerfeld enhanced cross section, $\sigma v_{\gamma\gamma}$ for the process, $F_1^0 F_1^0 \rightarrow \gamma\gamma$. At tree-level, this process does not take place because the DM is charge neutral but due to the multiple exchange of gauge bosons i.e W^\pm , Z and γ and charged states, $F_1^{(\pm Q)}$ in the ladder diagrams, the effective coupling with the photons is possible when the DM is non-relativistic. If $\epsilon_\phi \gtrsim 1$ and/or $\epsilon_v \gtrsim 1$, the Sommerfeld enhancement will be suppressed and in that case, $F_1^0 F_1^0 \rightarrow \gamma\gamma$ proceeds through one-loop process that gives, for 1-50 TeV mass range, $\sigma v_{\gamma\gamma}$ of the order $10^{-28} - 10^{-31} \text{ cm}^3 \text{ s}^{-1}$. Again, we can see from Fig. 8 that apart from some dips, for almost all of 1-20 TeV mass range, H.E.S.S. (orange dashed line) can exclude the DM in case of 5-plet (red line) and 7-plet (black line) using gamma-line searches.

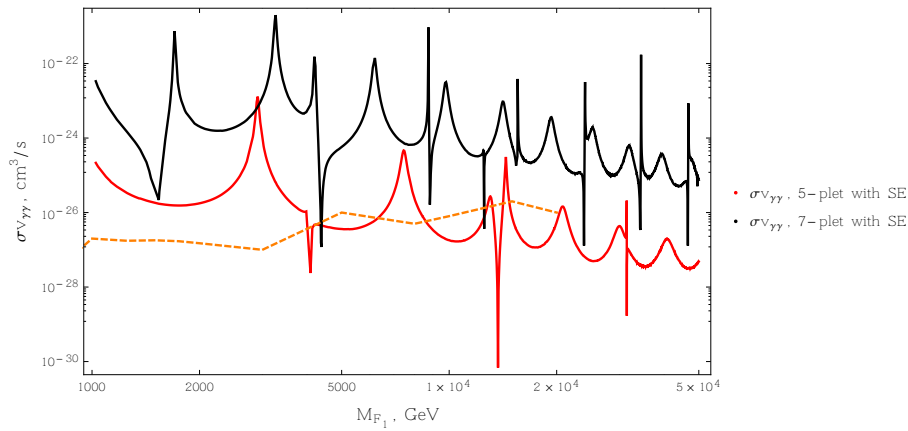


FIGURE 8: Sommerfeld enhanced $\sigma v_{\gamma\gamma}$ at the galactic halo of the Milky Way for 5-plet (red) and 7-plet (black). Here the orange dashed line is H.E.S.S. observed limit on $\sigma v_{\gamma\gamma}$.

In passing, we would like to point out that, unlike the case of scalar DM with larger electroweak multiplet which is focused in [17], the mass splittings among the fermionic component fields do not suppress the Sommerfeld enhancement as they are nearly degenerate for $\mathcal{O}(\text{TeV})$ mass range.

6. CONCLUSION AND OUTLOOK

From the present investigations on the Scotogenic model and the generalized KNT model with large electroweak multiplets, we can infer that in both models with scalar and fermionic DM, respectively, the Sommerfeld enhanced cross sections increase with the

size of the multiplets. In the case of the Scotogenic model, we have seen from Fig. 6 that larger multiplet like the quartet give rise to larger SE annihilation cross-sections compared to the smallest representation, the doublet and it is within the reach of H.E.S.S. and CTA limits.

Similarly for the generalized KNT model with 5-plet and 7-plet, we can see from Fig. 7 and Fig. 8 that for almost all of mass range, 1-50 TeV, the constraints from H.E.S.S. can exclude the F_1^0 being the DM, provided it is the dominant DM component and follows the Einasto density profile in both cases of 5-plet and 7-plet. That leaves only the singlet and triplet case as a viable DM candidate in the generalized KNT model. The singlet fermion, N_{R_1} of the KNT model which is electroweak neutral, does not receive any Sommerfeld enhancement. On the other hand, the triplet case, where the DM candidate is the neutral component of the fermion multiplet with isospin, $j = 1$, will have enhanced annihilation processes due to exchange of electroweak bosons but being smaller representation than the 5-plet or 7-plet, it may have larger portion of parameter space yet to be excluded by the H.E.S.S. limit but will be within the reach of future CTA sensitivity limits.

ACKNOWLEDGEMENTS

T.A.C would like to thank Shaaban Khalil and the organisers of BSM-2017 for the invitation and hospitality.

References

- [1] H. Abdallah *et al.* [HESS Collaboration], Phys. Rev. Lett. **117**, no. 11, 111301 (2016) [arXiv:1607.08142 [astro-ph.HE]].
- [2] H. Abdalla *et al.* [HESS Collaboration], Phys. Rev. Lett. **117**, no. 15, 151302 (2016) [arXiv:1609.08091 [astro-ph.HE]].
- [3] B. S. Acharya *et al.* [Cherenkov Telescope Array Consortium], arXiv:1709.07997 [astro-ph.IM].
- [4] E. Ma, Phys. Rev. D **73**, 077301 (2006) [hep-ph/0601225].
- [5] L. M. Krauss, S. Nasri and M. Trodden, Phys. Rev. D **67** (2003) 085002 [hep-ph/0210389].
- [6] Y. Cai, J. Herrero-Garcia, M. A. Schmidt, A. Vicente and R. R. Volkas, Front. in Phys. **5** (2017) 63 [arXiv:1706.08524 [hep-ph]].
- [7] T. A. Chowdhury and S. Nasri, JHEP **1512**, 040 (2015) [arXiv:1506.00261 [hep-ph]].
- [8] S. S. AbdusSalam and T. A. Chowdhury, JCAP **1405**, 026 (2014) [arXiv:1310.8152 [hep-ph]].
- [9] C. S. Chen, K. L. McDonald and S. Nasri, Phys. Lett. B **734** (2014) 388 [arXiv:1404.6033 [hep-ph]].
- [10] A. Ahriche, C. S. Chen, K. L. McDonald and S. Nasri, Phys. Rev. D **90** (2014) 015024 [arXiv:1404.2696 [hep-ph]].
- [11] A. Ahriche, K. L. McDonald and S. Nasri, JHEP **1410** (2014) 167 [arXiv:1404.5917 [hep-ph]].
- [12] A. Ahriche, K. L. McDonald, S. Nasri and T. Toma, Phys. Lett. B **746** (2015) 430 [arXiv:1504.05755 [hep-ph]].
- [13] T. A. Chowdhury and S. Nasri, Phys. Rev. D **97** (2018) no.7, 075042 [arXiv:1801.07199 [hep-ph]].
- [14] M. Cirelli, N. Fornengo and A. Strumia, Nucl. Phys. B **753** (2006) 178 [hep-ph/0512090].
- [15] C. Patrignani *et al.* [Particle Data Group], Chin. Phys. C **40** (2016) no.10, 100001.
- [16] M. Beneke, C. Hellmann and P. Ruiz-Femenia, JHEP **1505**, 115 (2015) [arXiv:1411.6924 [hep-ph]].
- [17] T. A. Chowdhury and S. Nasri, JCAP **1701**, no. 01, 041 (2017) [arXiv:1611.06590 [hep-ph]].
- [18] P. A. R. Ade *et al.* [Planck Collaboration], Astron. Astrophys. **594**, A13 (2016) [arXiv:1502.01589 [astro-ph.CO]].
- [19] T. Hambye, F.-S. Ling, L. Lopez Honorez and J. Rocher, JHEP **0907** (2009) 090 [JHEP **1005** (2010) 066] [arXiv:0903.4010 [hep-ph]].
- [20] J. Hisano, S. Matsumoto, M. Nagai, O. Saito and M. Senami, Phys. Lett. B **646**, 34 (2007) [hep-ph/0610249].
- [21] T. Cohen, M. Lisanti, A. Pierce and T. R. Slatyer, JCAP **1310**, 061 (2013) [arXiv:1307.4082].
- [22] C. Garcia-Cely, M. Gustafsson and A. Ibarra, JCAP **1602**, no. 02, 043 (2016) [arXiv:1512.02801 [hep-ph]].
- [23] J. Giedt, A. W. Thomas and R. D. Young, Phys. Rev. Lett. **103**, 201802 (2009) [arXiv:0907.4177 [hep-ph]].
- [24] E. Aprile *et al.* [XENON Collaboration], Phys. Rev. Lett. **119**, no. 18, 181301 (2017) [arXiv:1705.06655 [astro-ph.CO]].
- [25] D. S. Akerib *et al.*, arXiv:1608.07648 [astro-ph.CO].
- [26] E. Aprile *et al.* [XENON Collaboration], JCAP **1604**, no. 04, 027 (2016) [arXiv:1512.07501 [physics.ins-det]].
- [27] M. Klasen, C. E. Yaguna and J. D. Ruiz-Alvarez, Phys. Rev. D **87**, 075025 (2013) [arXiv:1302.1657 [hep-ph]].